High pressure Raman spectroscopic study on the relaxor ferroelectric $PbSc_{0.5}Nb_{0.5}O_3$

2009 J. Phys.: Condens. Matter 21 235901

(http://iopscience.iop.org/0953-8984/21/23/235901)

J. Phys.: Condens. Matter **21** (2009) 235901 (6pp) doi:10.1088/0953-8984/21/23/235901

High pressure Raman spectroscopic study on the relaxor ferroelectric $PbSc_{0.5}Nb_{0.5}O_3$

A-M Welsch[1,4], B Mihailova[1,4], M Gospodinov[2], R Stosch[3], B Güttler[3] and U Bismayer[1]

[1] Mineralogisch-Petrographisches Institut, Grindelallee 48, Universität Hamburg, D-20146 Hamburg, Germany
[2] Institute for Solid State Physics, Bulgarian Academy of Sciences, Boulevard Tzarigradsko Chausse 72, 1784 Sofia, Bulgaria
[3] Physikalisch-Technische Bundesanstalt, Bundesallee 100, D-38116 Braunschweig, Germany

E-mail: anna.maria.welsch@mineralogie.uni-hamburg.de, boriana.mihailova@uni-hamburg.de, crystlab@issp.bas.bg, Rainer.Stosch@ptb.de, Bernd.Guettler@ptb.de and mi4a001@uni-hamburg.de

Received 17 February 2009, in final form 8 April 2009
Published 15 May 2009
Online at stacks.iop.org/JPhysCM/21/235901

Abstract
The pressure evolution of the local structure and dynamics of polar nanoregions in $PbSc_{0.5}Nb_{0.5}O_3$ relaxor ferroelectric is analysed by Raman spectroscopy. The pressure dependence of phonon modes up to 10 GPa reveals three characteristic pressures related to changes in the local structure: near 2 GPa, at which ferroic ordering in the Pb system occurs; near 4 GPa, at which significant structural transformations, involving decoupling of Pb and B-cations in polar nanoclusters and suppression of the B-cation off-centring take place; and near 6 GPa, at which the system reaches a saturation state. The structural transformations observed in $PbSc_{0.5}Nb_{0.5}O_3$ are compared to those in $PbSc_{0.5}Ta_{0.5}O_3$ and other Pb-based perovskite-type relaxor ferroelectrics.

1. Introduction

Relaxors form a special group of ferroelectric materials that exhibits strong dielectric permittivity ε in a relatively large temperature range close to room temperature and considerable nanoscale structural inhomogeneity. Unlike normal ferroelectrics, they are characterized by a broad diffuse phase transition over a temperature range, strong frequency dispersion of ε as a function of temperature and weak remnant polarization [1]. Lead-based perovskite-type relaxors with the general formula $Pb(B', B'')O_3$ are very appealing for various technological applications [1]. In recent years there has been an enhanced interest towards studying their structure because of the outstanding piezoelectric and electro-optic properties of solid solutions of such relaxors and $PbTiO_3$ [2, 3]. The relaxor structure comprises two types of ordered/disordered states: (i) existence of polar nanoregions within a paraelectric matrix and (ii) existence of chemically B-site ordered nanoregions inside a B-site disordered matrix [4, 5]. The polar nanoregions occur at temperatures well above the temperature of the dielectric permittivity maximum T_m and for canonical relaxors their development into ferroelectric domains at low temperatures is impeded. Besides, above and in the vicinity of T_m the polar nanoregions are of dynamical character, i.e. they create and annihilate with a life time of $\sim 10^{-5}$–10^{-6} s near T_m [6]. Although extensive work has been carried out on relaxors over the past decade, the interplay between nanoscale structural complexity and relaxor properties is still not clarified. Studies on relaxors for a long time consisted of analysing the temperature evolution of structure as well as the effect of the degree of chemical B-site order, additional types of A- and B-site cations and external electric field [5–8]. A new dimension of investigations has been opened with the development of high pressure (HP) experimental techniques. Pressure is a much stronger driving force than temperature and it significantly slows down the dynamical structural fluctuations. Hence,

[4] Authors to whom any correspondence should be addressed.

the pressure evolution of relaxors can provide deeper insight into intrinsic structural peculiarities. So far, HP studies on Pb-based perovskite-type relaxors have pointed to three main features: (i) according to dielectric experiments at moderate pressures (up to 1.5 GPa), pressure induces a crossover from normal to relaxor ferroelectric state [4, 9]; (ii) the x-ray diffuse scattering, typical of relaxors at ambient pressure and arising from the polar nanoclusters [10, 11] is suppressed at HP [12–14] (iii) the Raman scattering at HP is inconsistent with the cubic perovskite-type structure [13–16]. The pressure driven crossover has been assumed to result from a decrease in the correlation length between polar clusters under pressure and it was further speculated that at higher pressures relaxors will reach a paraelectric cubic state. However, Bokov *et al* [17] showed that a pressure-induced crossover may not occur in some relaxor-normal ferroelectric solid solutions, thus indicating that the assumption for eventual transition to cubic structure is oversimplified. Besides, the explanation that the suppression of x-ray diffuse scattering reflects the vanishing of ferroic displacements should be ruled out because the observed HP Raman scattering indicates an enhancement of coherent non-cubic atomic arrangements [13–16]. Recently, complementary x-ray diffraction (XRD) and Raman spectroscopic analyses on $PbSc_{0.5}Ta_{0.5}O_3$ (PST) as a model relaxor ferroelectric unambiguously revealed the occurrence of a pressure-induced continuous phase transition, involving softening of the structure when approaching the critical pressure from both sides [18]. Pressure inhibits the dynamical coupling between the Pb and B-cation systems in the existing polar nanoregions, which results in a suppression of the existing off-centring of the B-site cations and an increase in the coherence length of correlated Pb off-centre displacements [18]. The regression of off-centred shifts of B-site cations leads to fragmentation of ferroelectric regions, which in many perovskite-type compounds manifests itself as a pressure-induced crossover to a relaxor state. However, the HP state differs from cubic; pressure favours ordering of electronic lone pairs of Pb^{2+} cations [18], i.e. of correlated Pb off-centre shifts, which in some compounds may hinder the crossover to a relaxor state. Monte Carlo simulations showed that the observed x-ray diffuse scattering in relaxors is mostly related to off-centred shifts of Pb atoms [11]. Therefore, the pressure-enhanced ferroic ordering in the Pb system explains the significant suppression of the observed x-ray diffuse scattering. The diminishing of B-cation off-centred shifts may also contribute to the reduction of the diffuse scattering.

To further explore pressure-induced transformation processes in Pb-based perovskite-type relaxors we applied HP Raman spectroscopy on $PbSc_{0.5}Nb_{0.5}O_3$ (PSN). PSN is comparable to PST because of the same 1:1 B-site stoichiometry, which favours long-range B-site chemical ordering, the same ionic radius of the ferroelectrically active B-site cation ($r_i(Nb) = r_i(Ta) = 0.64$ Å [19]), i.e. the same tolerance factor $t = \frac{r_i(A)+r_i(O)}{\sqrt{2}(r_i(B)+r_i(O))}$ and the occurrence of long-range ferroelectric ordering at low temperature [20]. However, the temperature evolution of Raman scattering indicates some structural dissimilarities between PSN and PST: (i) at high-temperature PSN exhibits smaller incipient ferroic species related to coherent off-centred Pb shifts as compared to those in PST and (ii) at low temperature a substantial fraction of the PSN structure remains in a paraelectric state [8, 21], whereas PST is characterized by an abundance of large ferroelectric domains and additional lowering of the local rotational symmetry [8, 22]. In this paper we present our results on the pressure evolution of local structure and the dynamics in PSN studied by Raman scattering.

2. Experimental details

Cubic-shaped single crystals of PSN were synthesized using the high-temperature solution growth method by cooling from 1453 to 1173 K with a rate of 0.3 K h^{-1}. The stoichiometry and chemical homogeneity were verified by electron microprobe analysis (Camebax microbeam SEM system). According to in-house powder XRD studies (Philips X'Pert diffractometer), the average structure is primitive cubic ($Pm\bar{3}m$) at room temperature, while synchrotron single crystal XRD (F1 beamline at DESY/HASYLAB) showed an abundance of polar nanodomains and could resolve the presence of chemically B-site ordered regions with $Fm\bar{3}m$ symmetry [21].

For HP experiments ⟨100⟩-oriented plates were polished to a thickness of ∼50 μm and then samples of approximate size 50 × 50 × 50 μm^3 were cut from these plates. The HP measurements were conducted in a gas-membrane driven Diacell® μScopeDAC–RT(G) (EasyLab), using a mechanically drilled stainless steel gasket. A methanol–ethanol–water mixture in the ratio 16:3:1 was used as a pressure transmitting medium, which ensured hydrostatic conditions up to 10 GPa. The actual pressure values were determined by the shift of the R1 photoluminescence peak of ruby chips placed next to the sample [23].

Raman scattering measurements were performed with a Horiba Jobin-Yvon T64000 triple-grating spectrometer, using the 514.5 nm line of an Ar^+ laser. The spectra were collected in back-scattering geometry, with an Olympus BH2 microscope and 50× long-working distance objective. At each pressure, a background spectrum was collected and subsequently subtracted from the sample spectrum in order to eliminate possible artificial signals from the pressure medium. Then the spectra were temperature reduced to account for the Bose–Einstein occupation factor. The peak positions, full-widths-at-half-maximum (FWHMs) and integral intensities were determined by fitting the spectrum profiles with Lorentzian functions. The repeatability of the spectral features and trends was verified by measuring two different samples.

3. Results and discussion

Figure 1 represents the overall evolution of Raman scattering of PSN from ambient pressure to 9.3 GPa. The Raman spectra of Pb-based perovskite-type relaxors are commonly analysed in terms of $Fm\bar{3}m$ symmetry, having the following optical phonon modes at the centre of the Brillouin zone:

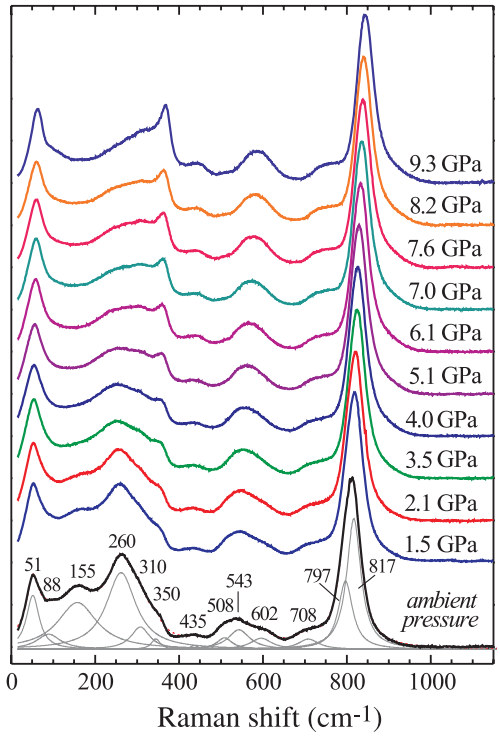

Figure 1. Raman spectra of $PbSc_{0.5}Nb_{0.5}O_3$ measured at different pressures. The fitting Lorentzians (grey thin lines) of the experimental spectrum measured at ambient pressure are also included in the plot; the resultant spectrum profile matches very well the experimental spectrum.

(This figure is in colour only in the electronic version)

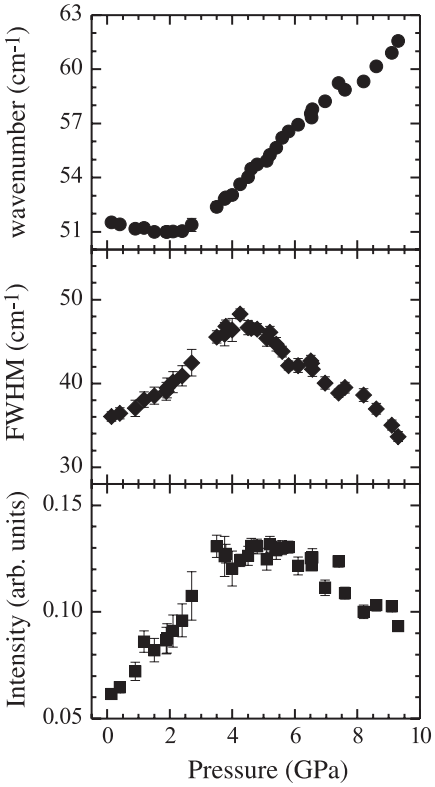

Figure 2. Pressure dependence of the wavenumber, FWHM and intensity of the Pb-localized F_{2g} mode near 51 cm^{-1}.

A_{1g} (Raman) + E_g(Raman) + $4F_{1u}$(infrared)+F_{1g}(inactive)+ F_{2u}(inactive) + $2F_{2g}$(Raman). Hence, the paraelectric cubic matrix contributes to four experimentally observed peaks, while the rest of the Raman signals result from vibrational modes in polar nanoregions. Due to the complexity of the structure, the observed Raman peaks are still controversially attributed to various cubic modes of the prototype structure [16, 24–26]. In the present study, we will follow the peak assignment used in [18], which is based on systematic studies of polarized Raman and infrared spectra of stoichiometric, A-site and B-site doped PST and PSN, measured at different temperatures [8, 22, 27–29]. There are two major ranges in the Raman spectra of PSN: between 400 and 900 cm^{-1}, which is dominated by internal BO_6 modes, and between 20 and 400 cm^{-1}, which is determined by modes involving heavy cation motions as well as rigid-unit (rotation and translation) BO_6 modes. As can be seen in figure 1, the latter spectral range is strongly affected by pressure. The pressure evolutions of the wavenumber ω, FWHM and integrated intensity for the Raman peak near 51 cm^{-1} are shown in figure 2. This peak is generated by the F_{2g} mode localized in Pb atoms [22], i.e. the amplitude of Pb atom displacements is considerable, while the vibration amplitude of the other types of atoms building the primitive unit cell (B-cations and oxygen atoms) is negligible [30][5]. As can be seen in figure 2, the wavenumber ω of the Pb-localized F_{2g} mode near 51 cm^{-1} as a function of pressure p exhibits a minimum at 2.2 GPa. An additional soft mode that appears in PST at nearly the same pressure is not resolvable for PSN, most probably due to the smaller size of the ferroic species with coherent off-centred Pb shifts. However, the $\omega(p)$-dependence clearly shows softening of the pseudocubic Pb-localized mode, thus indicating pressure-induced ferroelectric ordering in the Pb system, similarly to the case of PST. This is in agreement with the XRD data on PSN reported by Somayazulu [31], suggesting the occurrence of a phase transition at 2 GPa. However, the FWHM of the Pb-localized F_{2g} mode reaches its maximum at a higher pressure, at about 4 GPa, while the intensity has a broader maximum between 4 and 6 GPa (figure 2). Phonon modes involved in a phase transition experience substantial damping near the critical point because of the structural instability. Besides, in systems with dynamical structural fluctuations as in the case of relaxors, near the phase transition an increase in both FWHM and intensity of the lowest-energy mode is expected due to its coupling with the flip mode [32]. Thus, the pressure dependence of the width and intensity of the peak at 51 cm^{-1} indicates that most significant structural transformations in PSN take place near 4 GPa.

[5] The localization $L_S(t)$ of a certain mode S in a certain type of atoms t from the primitive unit cell can be quantitatively expressed by the ratio $L_S(t) = p_S(t)/\sum_t p_S(t)$ where $p_S(t)$ is the so-called participation ratio introduced by Bell and Dean (see for example [30]) and represents the magnitude of the vector displacements of atoms of type t for a normal mode S.

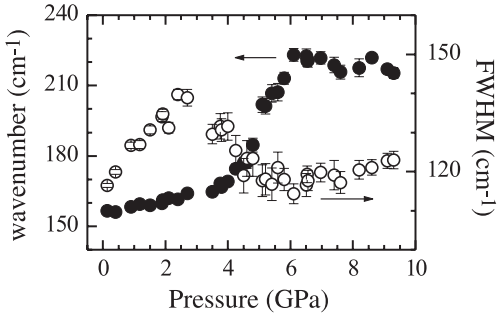

Figure 3. Wavenumber (filled symbols) and FWHM (open symbols) versus pressure for the Raman scattering near 155 cm^{-1} arising from Pb–BO_3 translation vibrations.

Further, we considered the Raman scattering near 155 and 260 cm^{-1}. Both signals arise from infrared-active F_{1u} modes of the prototype cubic structure and their appearance in the Raman spectra is due to the existing polar nanoregions. The phonon mode near 155 cm^{-1} comprises in-phase vibrations of the B-cation and oxygen atoms, which can be considered as a translation of the 'rigid' BO_3 group, as well as Pb vibrations opposite to the BO_3 motion. In the ideal perovskite-type structure with a primitive cubic cell this type of vibration is called the last mode [33]. In terms of rhombohedral symmetry, which is typical of the low-temperature state of perovskite-type relaxors, the Raman peak near 155 cm^{-1} results from a non-degenerate A-mode corresponding in frequency to the longitudinal F_{1u} cubic mode of the prototype structure. This assignment is in good accordance with the polar mode frequencies in $PbMg_{1/3}Nb_{2/3}O_3$ determined by infrared reflectivity spectroscopic analysis [34]. In the case of PST, a splitting of this mode was observed upon pressure, which indicates the suppression of the dynamical coupling between the off-centred Pb and B-site cations [18]. No apparent splitting of this mode was observed for PSN, which is most probably due to the smaller size and fraction of polar nanoregions as compared to PST [8]. However, the width of the Pb–BO_3 translation mode increases near 2.5 GPa, i.e. close to the characteristic pressure at which softening of the Pb-localized F_{2g}-mode is observed (figure 2). Besides, the Pb–BO_3 mode wavenumber dependence on pressure for PSN (see figure 3) resembles that observed for PST [18], indicating the occurrence of similar phenomena in both compounds. Hence, we assume that decoupling of the Pb and B-cation systems in polar nanoregions occurs in PSN as well. The $\omega(p)$-trend suggests that this process abundantly takes place above 4 GPa, where $d\omega(p)/dp$ of the Pb–BO_3 translation mode rapidly increases. This is in accordance with observed structural instability at about 4 GPa revealed by the maximum of the FWHM of the Pb-localized F_{2g} mode (figure 2). Near 6 GPa the $\omega(p)$ dependence of the Pb–BO_3 translation mode becomes nearly constant, showing that the transformation processes attain a saturation state.

The pressure evolution of the Raman scattering near 260 cm^{-1}, which arises from the B-cation-localized mode in polar nanoregions, also points out that 4 and 6 GPa are characteristic pressures (see figure 4). The pressure dependence

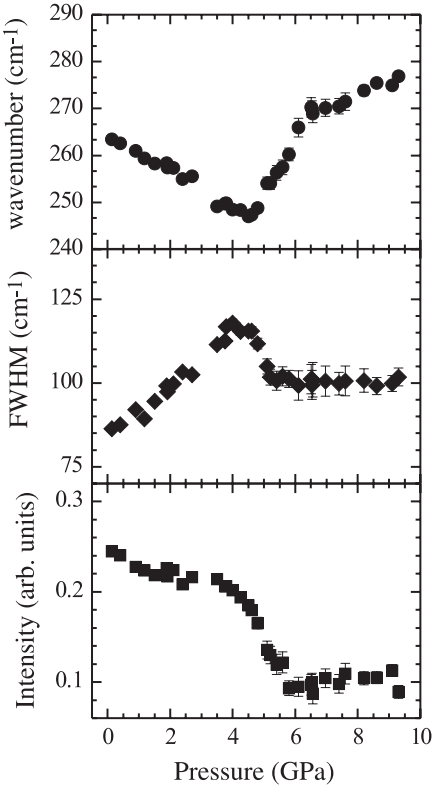

Figure 4. Pressure dependence of the wavenumber, FWHM and intensity of the B-cation-localized F_{1u} mode near 260 cm^{-1}, which is observable in Raman spectra due to the presence of off-centred displacements of the B-cations from their cubic positions.

of the wavenumber and FWHM shows, respectively, softening and damping of the mode at 4 GPa. At this pressure a drop in the intensity of the B-localized mode occurs, which reveals massive movement of the B-site cations back to the octahedral centres. At 6 GPa the intensity and FWHM reach a constant value, suggesting a completion of the corresponding structural changes. A pressure-induced decrease in the Raman scattering intensity near 250 cm^{-1} is typical of all perovskite-type relaxors studied [13, 16, 18] and, therefore, the suppression of off-centred displacements of B-cations is a characteristic structural feature of the HP state of relaxors. The intensity decrease is not so well pronounced for relaxor-$PbTiO_3$ solid solutions [14, 15], which indicates that the addition of $PbTiO_3$ stabilizes the B-cation off-centring.

Figure 5 presents the pressure dependence of the wavenumber and intensity of the Raman scattering near 350 cm^{-1}. This signal is associated with the silent F_{2u} mode of the prototype cubic structure, which involves Pb–O bond stretching vibrations, and its appearance in the Raman spectra is due to coherent off-centred shifts of Pb atoms with respect to the oxygen atom planes perpendicular to the cubic body diagonal [27]. The $\omega(p)$-dependence of this peak has a kink near 2 GPa, which corresponds well to the minimum of $\omega(p)$ of the Pb-localized F_{2g} mode near 51 cm^{-1} and also points to structural transformations in the Pb system. The increase in the Raman intensity near 350 cm^{-1} is enhanced above 4 GPa, i.e. when the suppression of off-centred

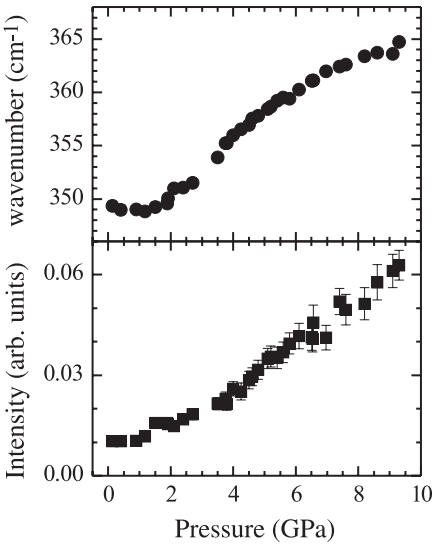

Figure 5. Pressure dependence of the wavenumber and intensity of the Raman scattering near 350 cm^{-1}.

B-cation displacements takes place. Therefore, the PSN structure responds to external elastic fields via enhancement of the ferroicity in the Pb–O system. The same pressure-induced increase in the Raman intensity near 350 cm^{-1} is observed for all Pb-based perovskite-type relaxors and related solid solutions [13–16, 18]. Hence, the pressure-enhanced enlargement of the coherence length of off-centred Pb shifts is a common structural feature for that class of materials.

The most evident pressure-induced change in the internal octahedral modes (see figure 1, the range 400–900 cm^{-1}) is observed for the symmetrical bending mode of BO_6 octahedra (F_{2g} in $Fm\bar{3}m$). At ambient pressure this mode gives rise to two components at 508 and 543 cm^{-1} due to the presence of rhombohedrally distorted BO_6 species in polar nanoregions and consequent splitting of the triple-degenerate mode to one non-degenerate and one double-degenerate mode. At pressures above 3.5 GPa a second, lower-wavenumber component is not required in order to rationally fit the spectrum profile. This indicates that at high pressure the BO_6 octahedra are 'more regular' regarding the values of O–B–O bond angles.

4. Conclusions

The pressure evolution of the Raman scattering of PSN up to 10 GPa reveals three characteristic pressures, $p_1 \sim 2$ GPa, $p_2 \sim 4$ GPa and $p_3 \sim 6$ GPa, at which the local structure undergoes transformations. The first pressure is associated with ferroic ordering processes in the Pb–O system, which, however, cannot be followed by the existing off-centred B-cations, triggering structural instabilities. As a result, at the second characteristic pressure massive structural changes take place, which involve violation of the dynamical coupling between the off-centred Pb and B-cations and consequent movement of the B-cations back to the octahedral centres. At the third pressure the suppression of B-cation off-centred shifts reaches saturation and upon further mechanical load the structure relaxes mainly via enlargement of the size and fraction of Pb–O ferroic clusters.

The comparison between PSN and PST shows that the replacement of Ta by Nb increases the characteristic pressure at which the decoupling of the Pb and B-cation systems in polar nanoregions and consequent suppression of B-cation off-centred shifts occurs. This indicates that ferroic Pb–O–Nb atomic linkages are more stable than the corresponding Pb–O–Ta linkages. Ferroic ordering in the Pb system takes place at nearly the same pressure for both compounds. For PST this structural transformation is revealed by the appearance of a soft mode, whereas for PSN it is manifested by the softening and damping of the Pb-localized Raman-active cubic mode. In the case of PSN, the decoupling of the Pb and B-cation systems in polar nanoregions happens at a pressure higher than the pressure of ferroic ordering of the Pb system, while the two transformation events take place at nearly the same pressure for PST. This distinction between the two compounds is most probably due to the difference in the stiffness of the Pb–O–B linkages and B-cation masses.

Acknowledgments

Financial support by the Deutsche Forschungsgemeinschaft (MI 1127/2-1) and Bulgarian Ministry of Education and Science (BY-X-308) is gratefully acknowledged.

References

[1] Bhalla A S, Guo R and Roy R 2000 *Mater. Res. Innov.* **4** 3
[2] Park S E and Shrout T R 1997 *J. Appl. Phys.* **82** 1804
[3] Li Y, Cheng Z-Y, Barad Y and Zhang Q M 2001 *J. Appl. Phys.* **89** 5075
[4] Samara G A and Venturini E L 2006 *Phase Transit.* **79** 21
[5] Hirota K, Wakimoto S and Cox D E 2006 *J. Phys. Soc. Japan* **75** 111006
[6] Blinc R, Gregorovič A, Zalar B, Pirc B, Laguta V V and Glinchuk M D 2000 *Phys. Rev.* B **63** 024104
[7] Toulouse J, Jiang F and Svitelskiy O 2005 *Phys. Rev.* B **72** 184106
[8] Mihailova B, Gospodinov M, Güttler B, Stosch R and Bismayer U 2007 *J. Phys.: Condens. Matter* **19** 275205
[9] Venturini E L, Grubbs R K, Samara G A, Bing Y and Ye Z-G 2006 *Phys. Rev.* B **74** 064108
[10] Xu G Y, Zhong Z, Bing Y, Ye Z G and Shirane G 2006 *Nat. Mater.* **5** 134
[11] Welberry T R and Goossens D J 2008 *J. Appl. Crystallogr.* **41** 606
[12] Chabaane B, Kreisel J, Dkhil B, Bouvier P and Mezouar M 2003 *Phys. Rev. Lett.* **90** 257601
[13] Janolin P-E, Dkhil B, Bouvier P, Kreisel J and Thomas P A 2006 *Phys. Rev.* B **73** 094128
[14] Ahart M, Cohen R E, Struzhkin V, Gregoryanz E, Rytz D, Prosandeev A, Mao H and Hemley R J 2005 *Phys. Rev.* B **71** 144102
[15] Chabaane B, Kreisel J, Bouvier P, Lucazeau G and Dkhil B 2004 *Phys. Rev.* B **70** 134114
[16] Kreisel J, Dkhil B, Bouvier P and Kiat J-M 2002 *Phys. Rev.* B **65** 172101
[17] Bokov A A, Hilczer A, Szafranski M and Ye Z-G 2007 *Phys. Rev.* B **76** 184116

[18] Mihailova B, Angel R J, Welsch A-M, Zhao J, Engel J, Paulmann C, Gospodinov M, Ahsbahs H, Stosch R, Güttler B and Bismayer U 2008 *Phys. Rev. Lett.* **101** 017602
[19] Shannon R D and Prewitt C T 1969 *Acta. Crystallogr.* B **25** 925 Shannon R D 1976 *Acta. Crystallogr.* A **32** 751
[20] Setter N and Cross L E 1980 *J. Appl. Phys.* **51** 4356
[21] Maier B, Mihailova B, Paulmann C, Ihringer J, Gospodinov M, Stosch R, Güttler B and Bismayer U 2009 *Phys. Rev.* B at press
[22] Mihailova B, Maier B, Paulmann C, Malcherek T, Ihringer J, Gospodinov M, Stosch R, Güttler B and Bismayer U 2008 *Phys. Rev.* B **77** 174106
[23] Munro R G, Piermarini G J, Block S and Holzapfel W B 1984 *J. Appl. Phys.* **57** 165
[24] Siny I G, Katiyar R S and Bhalla A S 2000 *Ferroelectr. Rev.* **2** 51
[25] Jiang F, Kojima S, Zhao C and Feng C 2001 *Appl. Phys. Lett.* **79** 3938
[26] Hehlen B, Simon G and Hlinka J 2007 *Phys. Rev.* B **75** 052104
[27] Mihailova B, Bismayer U, Güttler B, Gospodinov M and Konstantinov L 2002 *J. Phys.: Condens. Matter* **14** 1091
[28] Mihailova B, Bismayer U, Güttler B, Gospodinov M, Boris A, Bernhard C and Aroyo M 2005 *Z. Kristallogr.* **220** 740
[29] Mihailova B, Gospodinov M, Güttler B, Petrova D, Stosch R and Bismayer U 2007 *J. Phys.: Condens. Matter* **19** 246220
[30] Bell R J 1976 *Methods Comput. Phys.* **15** 215
[31] Somayazulu M, Ahart M, Cohen R and Hemley R 2008 *APS March Mtg(March 2008)*; *Proc. Am. Phys. Soc.* abstract #S37.009 http://meetings.aps.org/Meeting/MAR08/Event/79895
[32] Salje E, Devarajan V, Bismayer U and Guimaraes D M C 1983 *J. Phys. C: Solid State Phys.* **16** 5233
[33] Hlinka J, Petzelt J, Kamba S, Noujni D and Otsapchuk T 2006 *Phase Transit.* **79** 41
[34] Hlinka J, Otsapchuk T, Noujni D, Kamba S and Petzelt J 2006 *Phys. Rev. Lett.* **96** 027601